J. ISSS Vol. 3 No. 1, pp. 1-7, March 2014.

REGULAR PAPER

Molecular Dynamics Simulation of Residual Stress in a Si Quantum Dot Embedded in SiO_2

Bhamy Maithry Shenoy[a] , Gopalkrishna M. Hegde[b*] and D. Roy Mahapatra [a]

[a]Department of Aerospace Engineering, Institute of Science, Bangalore 560012, India

[b] Centre for Nano Science and Engineering, Indian Institute of Science, Bangalore 560012, India

* Corresponding author: gopal.hegde@gmail.com

Keywords:

Si, SiO_2, quantum dot, molecular dynamics simulation, residual stress, annealing, quenching, virial stress.

Abstract

Deformation plays a fundamental role in determining the properties of nano scale systems, for example in electronic energy band structures. A method to compute the residual stress distribution in nano-crystalline silicon (nc-Si) quantum dots embedded in an amorphous silicon dioxide (a-SiO_2) matrix using molecular dynamic simulations has been developed. In order to understand the process of formation and stabilization of quantum dots, we consider two different processes of cooling. In one case, a quenching condition is applied, and, in another case, a slow annealing condition is applied. Atomic level stresses are calculated using the virial theory. It is observed from the simulation results that cooling rates significantly affect the residual stress distribution. Quenching produces a high density of defects in the crystalline core as well as in the diffused interface region, whereas annealing reduces the density of defects and gives a very well defined interface region between the crystalline Si core and amorphous SiO_2 shell. Further, annealing produces compressive stress close to the interface region similar to the experimental observations reported earlier. Altering the defect distribution is a potential approach to designing optimal energy band structures.

1. Introduction

Microelectronics is dominated by silicon technology. At present, optoelectronic devices are made of III-V semiconductors. They introduce undesirable local strains during integration with Si microelectronic devices due to a different lattice property. However, bulk silicon is not suitable in optoelectronics as it does not emit photoluminescence in the visible region. This is because it has an indirect band gap where phonon-assisted non-radiative transitions are favored over radiative transitions. The desire for the integration of optoelectronic devices with microelectronics has triggered a search for light-emitting Si-based materials. Si nanostructures such as porous silicon and nano-crystalline Si embedded in an insulating matrix are promising candidates since they emit visible photoluminescence [Parvesi *et al* 2000, Ball 2001, Kanemitsu *et al*. 1993 and 2000]. The origin of photoluminescence in such nanostructures has been under intense debate. Whether it is due to the quantum confinement of excitons [Kanemitsu *et al*. 1993 and 2000] or defects at the Si/SiO_2 interface [Godefroo *et al*. 2008] is still an open question. A clear understanding of the structure at

Available online at www.isssonline.in/journal/03paper01.pdf Paper presented at the Fifth ISSS National Conferece on MEMS, Smart Materials, Structures and Systems, September 21-22, 2013 (ISSS NC 5), Karpagam University, Coimbatore, India.

the atomistic level may help resolve this issue. Various other applications of Si nanostructures include a third generation of photovoltaic cells, [Green 2003] single electron transistors as a basic element in VLSI design, [Zaknoon *et al*.2008] and others (see [Koshida 2008] for various other applications of Si nanostructures).

The properties of Si based devices can be modulated due to various reasons such as impurities, dislocations, stress, [Kohno *et al*. 2002, Arguirov *et al*. 2006, Kahler *et al*. 2000, Dhara *et al*. 2011] etc. For instance, a stress field greater than 12 GPa modifies the band structure of bulk Si from the indirect to the direct band gap [Karazhanov *et al*. 2008]. At the nano-scale, the magnitude of stress is estimated to be in the range of 25-50 GPa [Karazhanov *et al*. 2008].

Several studies have been reported earlier on the stress distribution in nc-Si embedded in SiO_2 systems, both using the atomistic approach [Hadjisavvas *et al*. 2004, Guerra 2009] and the continuum approach [Thean *et al*. 2001]. Guerra [Guerra 2009] considered a crystalline Si core with a diamond-like structure having in-built tensile strain. The SiO_2 shell was assumed to have a β-crystobalite structure. The interface between the crystalline Si core and the SiO_2 shell was assumed to have no defects. Hadjisavvas *et al*. [2004] started with a pre-strained Si core having a diamond crystal structure and a SiO_2 shell with μ-crystobalite. In order to produce an amorphous structure in the shell, the initial structure was subjected to repeated quenching with with constrain that the Si atoms in the crystalline core do not move. These studies have, however, ignored the fabrication conditions that give rise to residual stress. The inbuilt stress in nanostructures is referred to as residual stress. Residual stresses are mostly due to lattice mismatches and a difference in the thermal expansion coefficient between various materials. They are inbuilt in the fabricated structures and are different from instantaneous stresses which are induced during phonon vibrations and external applications. The fabrication of nc-Si/a-SiO_2 quantum dots involves annealing in N_2 ambient at 1000^0C for reducing defects such as Si dangling bonds at the interface region [Hirano *et al*. 2001, Kosowsky *et al* 1997].

The objective of this work is to develop a method to compute residual stress developed in nc-Si embedded in a SiO_2 matrix due to annealing by using molecular dynamic simulations. The modeling and simulation procedure is described in Section 2. Section 3 presents the results and discussions. Conclusions are given in section 4.

Molecular Dynamic Modelling

2.1 Interatomic Potential:

In the present work, the Tersoff potential of Munetoh [Munetoh *et al*. 2007] has been considered for the Si, O mixed system. The Tersoff potential [Hirano *et al*. 2001] is an empirical function composed of two- and three-body terms depending on the local environment. The two body term describes the interactions between atoms. The three-body term is included to describe angular contributions to the forces due to bond angles in covalent systems. The total potential energy E can be written as

$$E = \sum_i E_i = \frac{1}{2}\sum_{i\neq j,j=1}^{N} V_{ij} \quad (1)$$

$$V_{ij} = f_C(r_{ij})[f_R(r_{ij}) + b_{ij} f_A(r_{ij})] \quad (2)$$

where E_i is the site energy and V_{ij} is the bond energy. The indices i and j run over the atoms of the system and r_{ij} is the bond length between the atoms i and j. is the sum of a repulsive pair potential (f_R) and an attractive pair potential (f_A). The repulsive term includes orthogonalization energy when atomic wavefunctions overlap. The attractive term is associated with the bonding. f_C is merely a smooth cut-off function to limit the range of the potential. The term represents a measure of bond order and is assumed to be a monotonically decreasing function of the coordination of atoms i and j. f_C, f_R, f_A and b_{ij} are expressed as

$$f_R(r_{ij}) = A_{ij} exp(-\lambda_{ij} r_{ij}) \quad (3)$$

$$f_A(r_{ij}) = B_{ij} exp(-\mu_{ij} r_{ij}) \quad (4)$$

$$f_R(r_{ij}) = \begin{cases} 1, & \text{for } r_{ij} < R_{ij} \\ \frac{1}{2} + \frac{1}{2}\cos\left(\pi \frac{r_{ij}-R_{ij}}{S_{ij}-R_{ij}}\right) & \text{for } R_{ij} < r_{ij} < S_{ij} \\ 0, & \text{for } r_{ij} > S_{ij} \end{cases} \quad (5)$$

$$b_{ij} = \chi_{ij}\left[1 + \beta_i^{n_i}\zeta_{ij}^{n_i}\right]^{-1/2n_i} \quad (6)$$

where *i*, *j*, and *k* denotes the atomic labels. A_{ij}, B_{ij}, λij and μ_{ij} are the parameters of the potential. R_{ij} and S_{ij} in equation (5) are chosen to include the first nearest neighbors. *Xij* in Eq. (6) is used for the weakening or strengthening of heteropolar bonds and accounts for the charge transfer between the atoms. ζij gives the effective co-ordination number of atom *i* and is expressed as

$$\zeta_{ij} = \sum_{k\neq i,j} f_C(r_{ik})\,\omega_{ik}\,g(\theta_{ijk}) \quad (7)$$

$$g(\theta_{ijk}) = 1 + \frac{c_i^2}{d_i^2} - \frac{c_i^2}{\left[d_i^2 + (h_i - \cos\theta_{ijk})^2\right]} \quad (8)$$

θ_{ijk} is the bond angle between the *ij* and *ik* bonds. ω_{ik} in Eq. (7) can permit greater flexibility when dealing with more drastically different types of atoms. The parameters for the Si-Si and Si-O interaction potential are tabulated in Table I. Further details can be found in references [Hirano *et al*. 2001, Munetoh *et al*. 2007].

Table 1: The optimized parameters for the Si–Si, Si–O and O–O interactions considered in the present work (taken from ref. [Munetoh *et al*. 2007])

	Si	O
A (eV)	1.8308×10^{3}	1.88255×10^{3}
B (eV)	4.7118×10^{2}	2.18787×10^{2}
λ (Å^{-1})	2.4799	4.17108
μ (Å^{-1})	1.7322	2.35692
β	1.10×10^{-6}	1.1632×10^{-7}
N	7.8734×10^{-1}	1.04968
C	1.0039×10^{5}	6.46921×10^{-1}
D	1.6217×10^{1}	4.11127
H	-5.9825×10^{-1}	-8.45922×10^{-1}
R (Å)	2.5	1.7
S (Å)	2.8	2.0
$\chi_{Si-O} = 1.17945$		

2.2 Modelling and Simulation Procedure

The structure is created based on the fabricated quantum dot structures reported in the literature. The quantum dot structure, as fabricated by various methods consists of a crystalline silicon core with a diamond crystal structure and an amorphous SiO_2 shell [Kahler *et al*. 2000, Scheer *et al*. 2003]. The initial quantum dot configuration for MD simulation was based on an experimentally grown structure reported in [Scheer *et al*. 2003] and is shown in figure 1. The quantum dot core is made of crystalline silicon having a diamond crystal structure. It consists of about 34,874 Si atoms and has a diameter of about 11.5 nm. The outer shell is 3 nm thick and is made of amorphous SiO_2 with Si and O atoms in the ratio of 1:2.048. The shell consists of about 1,13,851 atoms. The square base of a-SiO_2 having the same ratio of Si and O atoms as in the shell is of side 16 nm and 4 nm thick and consists of about 97,275 atoms. The total atoms in the MD simulation are approximately 2.46×10^5.

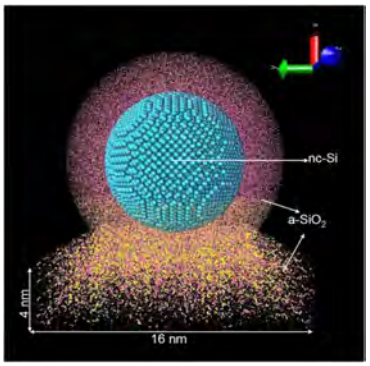

Figure 1: Initial nc-Si/a-SiO_2 quantum dot on a-SiO_2 base used for simulation.

The procedure of simulation is described in figure 2. The initial structure is first subjected to energy minimization using the conjugate gradient method. This structure is then subjected to thermal equilibration at a high annealing temperature of 1200 K using a Nose-Hoover (N-H) [Nosé 1984, Hoover 1985] thermostat for about 2 ps at a time step of 1fs. The structure is then subjected to energy minimization and later allowed to relax at room temperature for 10 ps. The effect of cooling rates on the residual stress distribution has been studied for two cases.

- Case A: (Quenching) The quantum dot system is cooled from a temperature of 1200 K to room temperature (300 K) rapidly using a N-H thermostat for about 12 ps at a time step of 1 fs. The cooling rate is 1 K/ps.
- Case B: (Annealing) The quantum dot system

is cooled from a temperature of 1200 K to room temperature (300 K) very slowly. The typical MD simulation is limited by about 10^3-10^6 time steps. So in order to decrease the effective cooling rate, the cooling rate was fixed at 1 K/ps, but in every intermediate step of a 100 K decrease in temperature, the structure was subjected to energy minimization and relaxation at that state for about 10 ps. This was done to ensure the experimental condition in which, during annealing, the system tries to reach a stable configuration at every intermediate temperature before finally reaching the room temperature.

The bottom of the base (about 2 nm) is fixed during the simulation in order to prevent the motion of the entire structure. This does not affect our objective as we are mostly interested in the Si/SiO--$_2$ interface properties. Also, in actual structures, the base is relatively very thick so that the bottom is fixed during dynamics. Periodic boundary conditions are applied along the y and z directions. The equations of motion are integrated using the velocity Verlet algorithm [Swope *et al*. 1982]. The atomic stress is the sum of a potential energy part and a kinetic energy part. The potential energy part depends on the atomic positions and inter-atomic forces and describes the continuum measure of the internal mechanical interactions between atoms. The dynamical or kinetic energy part represents the thermal stress that would develop in a constrained system subjected to a temperature change [Subramaniyan *et al*. 2008]. The stress component $\sigma^i_{\alpha\beta}$ for an atom *i* calculated using the virial theory is given by the expression [Subramaniyan *et al*. 2008]

$$\sigma^i_{\alpha\beta} = \frac{1}{\Omega_i}\left[\frac{1}{2}\sum_{j=1}^{N}(r^j_\alpha - r^i_\alpha)f^{ij}_\beta - m^i\,(v^i_\alpha - \bar{v}^i_\alpha)\left(v^j_\beta - \bar{v}^j_\beta\right)\right] \quad (9)$$

where (α, β) take the values of the x, y and z (directions), Ω_i is the volume of atom *i*, r^i_α (r^j_β) is the position of atom *i* (*j*) along α, f^{ij}_β is the force along β on atom due to atom *j*. It is equal to the negative gradient of the total potential energy E (given by equation (1)) with respect to the atomic position. is the mass of atom , is the velocity of atom and is the local average velocity. The quantity $(v^i_\alpha - \bar{v}^i_\alpha)$ represents the thermal excitation velocity of atom *i*.

The simulations are done using LAMMPS [2010]. For visualization we used J. Li's AtomEye [2003] and VMD [Humphrey *et al*. 1996].

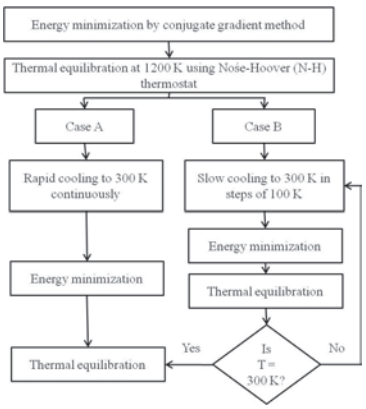

Figure 2: Flow chart of simulation procedure

3. Results and Discussion

The quantum dot is subjected to two different cases of cooling as described in section 2. The atomic stresses developed due to cooling are then computed from equation (9) for the structures at the end of each case of simulation. The atomic stress components computed here are in the units of GPa multiplied by the atomic volume. The figures 3-5 show atomic stress components on various planes for case A.

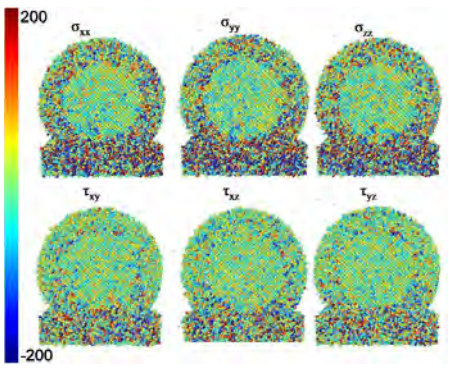

Figure 3: Atomic stress components for case A on xy plane

It is observed from figures 3-5 that the thin a-SiO_2 shell and the base layer have high density stress concentrations (defects). The comparatively larger crystalline Si core is slightly tensile. However, due to rapid cooling, the core also contains many defects. It is also observed that the interface region is not well formed but diffused. The principal components of stress have a higher magnitude than the shear components. It is to be noted here that, by defects we mean highly stressed atomic sites.

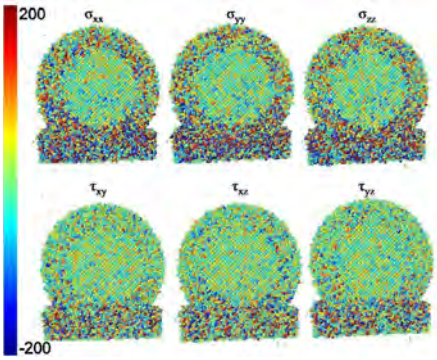

Figure 4: Atomic stress components for case A on xz plane

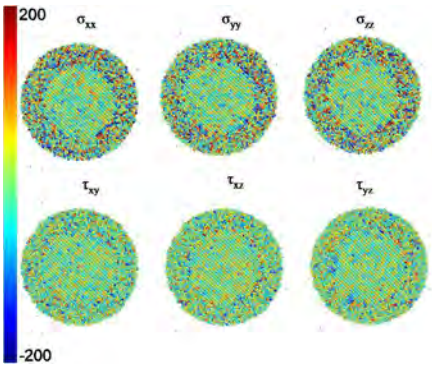

Figure 5: Atomic stress components for case A on yz plane.

High stress can exist when the atomic configuration deviates from the lowest energy state. This is either due to stretched/compressed bonds or missing atoms (point defects). The nature of defects at the interface is the subject of future studies. The focus of the present work is to set up a method to create Si quantum dot structures comparable to fabricated ones.

The atomic stress components on various planes for case B are plotted in figures 6-8.

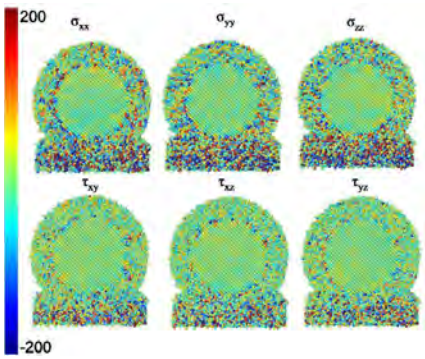

Figure 6: Atomic stress components for case B on xy plane.

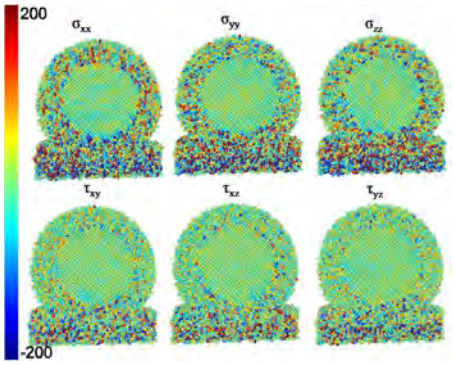

Figure 7: Atomic stress components for case B on xz plane.

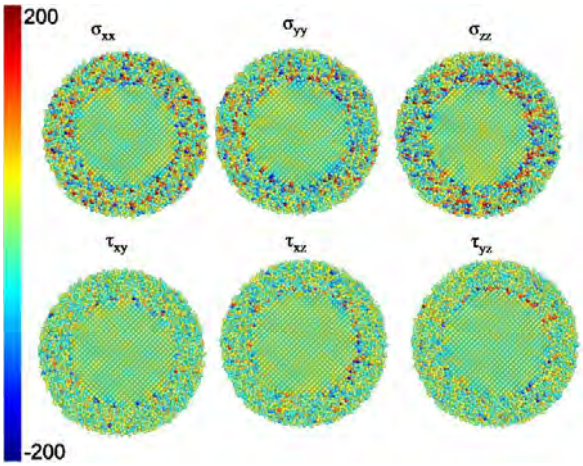

Figure 8: Atomic stress components for case B on yz plane.

As seen from figures 6-8, the density of defects in the entire structure is reduced significantly (nearly 80%) in case B with almost no defects in the core. This is in accordance with the well-known fact that annealing reduces stress in the system. Also, it is observed from figures 6-8 that the stress is mostly concentrated close to the interface between the crystalline Si core and the amorphous SiO_2 shell and has a compressive nature. Earlier reported studies have shown that high compressive stresses are observed close to the interface [Kosowosky *et al*. 1997]. From figures 6-8, it can be seen that the amorphous shell in case B is slightly compressively stressed. From the simulation results, we see that case B reproduces the trends observed experimentally. It is also to be noted here that earlier studies used Si cores with uniform tensile stress distribution and without any defects at the interface as an initial configuration for the band structure [Hadjisavvas *et al*. 2004,

Guerra 2009]. But from the present simulation and earlier reported studies [Kahler *et al*. 2000, Kosowosky *et al*. 1997], during annealing, non-uniform stress is generated with a high stress concentration near the interface.

4. Conclusions

We have developed a method based on molecular dynamic simulations to compute the residual stress distribution in an nc-Si/a-SiO_2 quantum dot structure on a-SiO_2 base. We have started with a realistic structure by considering an equilibrated structure which is then subjected to fabrication conditions. The residual stress distribution due to fabrication was studied considering two cases of cooling, namely case A (quenching) and case B (annealing). The simulations reveal that during quenching, a large density of defects is formed in the entire structure. The interface region becomes diffused. However, during annealing the defect density is reduced by 80% in the entire structure. The crystalline core is observed to be tensile and the shell is compressively stressed. The interface region is well formed and high compressive stress is formed close to the interface region. The residual stress distribution analysis presented in this work can be used to compute electronic energy levels more accurately. The present analysis is also very useful in semiconductor device fabrication particularly in MEMS and nanostructures.

Acknowledgements

The authors gratefully acknowledge financial support through the Computational Nano engineering Project under NPMASS Program, Govt. of India.

References

Arguirov, T., Mchedlidze, T., Kittler, M., Rölver, R., Bergoff, B., Först, M., and Spangenberg, B., 2006, Residual stress in Si nanocrystals embedded in a SiO_2 matrix, Appl. Phys. Lett., Vol. 89, 053111.

Ball, 2001, Let there be light, Nature, 409, 974-976.

Dhara and Giri, 2011, Size Dependent Anisotropic Strain and Optical Properties of Strained Si Nanocrystals, J. Nanosci. Nanotechnol., Vol. 11, 1–7.

Godefroo, S., Hayne, M., Jivanescu, M., Stesmans, A., Zacharias, M., Lebedev, O. I., Tendeloo, G. Van and Moshchalkov, V. V., 2008, Classification and control of the origin of photoluminescence from Si nanocrystals, Nature Nanotechnology, Vol. 3, 174-178.

Green, M. A., 2003, Third Generation Photovoltaics: Advanced Solar Energy Conversion, Kamiya, T., Monemar, B., Venghaus, H. and Yamamoto, Y., Berlin, Springer Berlin Heidelberg.

Guerra, 2009, Size, oxidation, and strain in small Si/SiO2 nanocrystals, Phys. Rev. B, Vol. 80, 155332.

Hadjisavvas and Kelires, P. C., 2004, Structure and Energetics of Si Nanocrystals Embedded in a-SiO_2, Phys. Rev. Lett., Vol. 93, 226104.

Hirano, Y., Sato, F., Aihara, S., and Saito, N., 2001, Photoconductive properties of nanometer-sized Si dot multilayers, Appl. Phys. Lett., Vol. 79, 2255-2257.

Hoover, W. G., 1985, Canonical dynamics: Equilibrium phase-space distributions, Phys. Rev. A, Vol. 31, 1695–1697.

Humphrey, W., Dalke, A. and Schulten, K., 1996, VMD - Visual Molecular Dynamics, J. Molec. Graphics, Vol. 14, 33-38. http://www.ks.uiuc.edu/Research/vmd/

Kahler, U, and Hofmeister, 2000, Synthesis of Si nanoparticles within buried layers of SiO_x, Material Science Forum, vols. 343-346 , 488-493, Journal of metastable and nanocrystalline materials, Vol. 8, 488-493.

Kanemitsu, Ogawa, Shiraishi, and Takeda, 1993, Visible photoluminescence from oxidized Si nanometer-sized spheres: Exciton confinement on a spherical shell, Phys. Rev. B, Vol 48, No. **7**, 4883-4887.

Kanemitsu, Y., Fukunishi, Y., Iiboshi, M., Okamoto, S., and Kushida, T., 2000, Visible luminescence from Si/SiO2 quantum wells and dots: confinement and localization of excitons, Physica E, Vol. **7**, 456-460.

Karazhanov, S. Zh., Davletova, A. and Ulyashin, A., 2008, Strain-induced modulation of band structure of silicon, J.of Appl.Phys., Vol. 104, 024501.

Kohno, H., Iwasaki, T., Mita, Y., and Takeda, S., 2002, One-phonon Raman scattering studies of chains of crystalline-Si nanospheres, J. Appl. Phys., Vol. 91, 3232-3235.

Koshida, N., 2008, Device Applications of Silicon Nanocrystals and Nanostructures, 1st ed., Koshida, N., Springer.

Kosowsky, S. D., Pershan, P. S., Krisch, K. S., Bevk, J., Green, M. L., Brasen, D., Feldman, L. C., and Roy, P. K., 1997, Evidence of annealing effects on a high-density Si/SiO2 interfacial layer , Appl. Phys. Lett., Vol. 70, 3119-3121.

LAMMPS (2010) http://www.cs.sandia.gov/~sjplimp/lammps.html

Li, J., 2003, AtomEye: an efficient atomistic configuration viewer, Modelling Simul. Mater. Sci. Eng., Vol. 11 173.

Munetoh, Shinji, Motooka, Moriguchi, and Shintani, 2007, Interatomic potential for Si–O systems using Tersoff parameterization, Computational Materials Science, Vol. 39, 334–339.

Nosé, S., A unified formulation of the constant temperature molecular dynamics methods, 1984, The Journal of Chemical Physics, Vol. 81, 511–519.

Pavesi, L., Negro, L. Dal, Mazzoleni, C., Franzò, G. and Priolo, F., 2000, Optical gain in silicon nanocrystals, Nature (London), 408, 440-444.

Scheer, K. C., Rao, R. A., Muralidhar, R., Bagchi, S., Conner, J., Perez, C., Sadd, M. and White, Jr., B.E., 2003, Thermal oxidation of silicon nanocrystals in O_2 and NO ambient, J. Appl. Phys., Vol. 93, 5637-5642.

Subramaniyan, A. K., and Sun, C. T., 2008, Continuum interpretation of virial stress in molecular simulations, International Journal of Solids and Structures, Vol. 45, 4340–4346.

Swope, W. C., Andersen, H. C., Berens, P. H., and Wilson, K. R., 1982, A computer simulation method for the calculation of equilibrium constants for the formation of physical clusters of molecules: Application to small water clusters, The Journal of Chemical Physics, Vol. 76, 637–649.

Thean and Leburton, J. P., 2001, Strain effect in large silicon nanocrystal quantum dots, Appl. Phys. Lett., Vol. 79, 1030.

Zaknoon, B, Bahir, G., Saguy, C., Edrei, R., Hoffman, A., Rao, R.A. , Muralidhar, R. and Chang, K-Mi, 2008, Study of single silicon QD band gap and single-electron charging energies by room temperature STM, Nanoletters, Vol. 8, 1689-1694.

Bhamy Maithry Shenoy received her M.Sc degree in Physics from Mangalore University in 2008. She is currently pursuing PhD in Indian Institute of Science, Bangalore. Her research interests include multi-physics modeling, material and process simulation of semiconductors at nano-scale.

Gopalkrishna Hegde received his M.Sc and Ph. D in Physics, all in India. He is currently with the Centre for Nano Science and Engineering, Indian Institute of Science, Bengaluru. He has over 100 publications in international journals and conference proceedings and has filed 4 patents. He has completed many sponsored research projects students in India and in Singapore. He has presented invited talks/key notes at various institutions and at international conferences. He was Visiting Professor in the FEMTO-ST Institute, Université de Franche-Comté, France (2013) Univ. of Rennes, France(2008). His current research interests are in the areas of photonics, optical sensors, optical flow visualization, micro-nanofabrication and microfluidics.

D Roy Mahapatra got his Ph.D. (Aerospace Engg.) Indian Institute of Science Bangalore (2004)B.E. (Civil Engg) Jadavpur University Kolkata (1998).Currently he is Associate Professor, Dept. of Aerospace Engg. Indian Institute of Science , Bengaluru.His research interests are: Mechanics of Materials, Materials and Structural Diagnostics,Wave Phenomena, Smart Sensors and Actuators,Systems Health Monitoring and Integration of Nano-Bio Engineering Systems.